Journal of Computation and Artificial Intelligence in Mechanics and Biomechanics ISSN 2184-8971
Volume 1, Issue 3, Page 81-91, 2021

Development of a DoE with a new electrospinning system for cartilage tissue engineering

Silva E. [1], Semitela A. [2], Marques P.A.A.P. [3], Completo A. [4]

[1] *eduardasilva@ua.pt; Universidade de Aveiro; Aveiro; Portugal*
[2] *angela.semitela@ua.pt; Universidade de Aveiro; Aveiro; Portugal*
[3] *paulam@ua.pt; Universidade de Aveiro; Aveiro; Portugal*
[4] *completo@ua.pt;Universidade de Aveiro; Aveiro; Portugal*

Abstract
Electrospinning is currently one of the most used techniques to produce fibrous synthetic tissues such as cartilage and bone. To replicate cartilage tissue engineering functionality, one of the most important characteristics is the alignment of the resulting fibre meshes in a three-dimensional (3D) fashion. Here, a newly developed electrospinning collector system is tested in order to understand how the process parameters affected the obtained fibre meshes topography. For that, a polymer consisting of PCL/Gelatin was electrospun using the electrostatic potential to create a fibre mesh. A Design of the Experiments (DoE) approach was implemented, to determine whether the variation of the main process parameters led to significant effects on the mesh dimensional characteristics. The process parameters analysed were the velocity of the collecting bands, the linear velocity of the fibre deposition table and the flow rate. The analysed mesh characteristics were the fibre diameter, the distance between the fibres and pore size. The effect of each of the three factors was statistically analysed using ANOVA, as well as the interaction between them. Complementary an ANOVA linear regression approach was developed to predict the distance between the fibres. This statistical regression was then compared with a predictive theoretical model and with the experimental results. The results obtained indicate the presence of interactions between the three process parameters analysed. The three process parameters showed statistical significance in the distance between the fibres, however, the velocity of the deposition table was the process parameter that presented the highest effect.

***DOI**: 10.5281/zenodo.5710429*

Article Info

Keywords
Electrospinning
Nanofiber alignment
Biomechanics
Tissue Engineering
Design of Experiments
Biofabrication
ANOVA

Article History
Received: *27/01/2021*
Revised: *05/04/2021*
Accepted: *14/05/2021*

1. Introduction

In the current days, one of the biggest challenges in cartilage tissue engineering (TE) is the difficulty to mimic the biomechanical environment of cartilage's native tissue [1-8]. So far, various biofabrication techniques have been used [1, 9-15], in which it was possible to develop artificial cartilage with similar biochemical properties to the native tissue. The main limitation remains on the fact that the artificial cartilage developed does not recapitulate the fibril zonal variances the native cartilage tissue does [1, 12-15]. The organization of the collagen fibrils through the depth of the cartilage tissue is extremely important and should be replicated in the artificial tissue for it to become mechanically functional [12-14, 16]. This can be achieved using anisotropic fibrous scaffolds since they allow mimicking the extracellular matrix (ECM) structure/organization of native tissues [11-14]. Electrospinning is a process for the development of polymer nanofibres [1, 5-6, 8] using electrostatic potential to create a continuous fiber that can be collected in the form of a mat. This technology has been widely used in the field of TE to produce synthetic tissue, such as cartilage [9-15]. However, it is necessary to find an efficient way to control the alignment of polymeric nanofibres matrices during the electrospinning process in order to mimic the topography of the native cartilage ECM [9-15]. In this study, a recently developed electromechanically electrospinning system [17] was employed on the fabrication of aligned nanofibres mats. This electrospinning platform has the capacity to control the fibre alignment as well as the distance between the aligned fibres and thus the scaffold pore size. The pore size, as the fibre diameter, are important factors affecting tissue regeneration efficiency [11-12]. Thus, an experiment plan (DoE) for the automated electrospinning system was developed in order to understand how the velocity of the collecting bands, the velocity of the deposition table and the flow rate would affect the dimensional characteristics of the resulting nanofibres mats, as the fibre diameter and pore size. Complementary, a mathematical model was developed capable of predicting the dimensional characteristics of the nanofibres mats, and the results compared with the experimental ones.

Corresponding Author:
António Completo
completo@ua.pt

2. Methods and Materials

2.1. Materials

Polymeric solutions of polycaprolactone (PCL; Sigma-Aldrich) and Gelatin from porcine skin (Sigma-Aldrich) were dissolved separately in 2,2,2-trifluoroethanol (TFE; TCI) at a concentration of 10 wt % and mixed in a 60:40 volume ratio, respectively, to be used throughout the entire experimental procedure. Previous studies have reported the use of that PCL blends to produce aligned nanofibres and to recreate cartilage's composition [11-12, 18]. PCL is a biodegradable polymer extensively used in TE due to its suitable tensile property and biocompatibility [9-15]. However, this polymer's hydrophobicity and slow biodegradation rate are restraints on its applications. Gelatin is a congener protein of collagen and is a widely utilized biomaterial [10-11]. However, its fast degradation time and its highly hydrophilic surface may not be appropriate as the base material. To overcome the respective limitations of these two materials and take each other's advantages, PCL/gelatin hybrid nanofibrous structures obtained by electrospinning have been successfully developed for biomedical applications [10-11].

2.2. Electrospinning System

A new electrospinning system was used [17] where the PCL solution was placed inside a syringe attached to a pump, which forms the emitter module (+20kV) of the system, as it can be seen in Fig. 1. Besides the emitter module, the system also contains a collecting and deposition module. The collecting module, also shown in Fig. 1, consists of two rotating, metallic bands (Band 1 and Band 2), that attract the electrospun fibres. The result is a fibre mat formed in the gap between the two bands, as shown in Fig. 1, the bands are the only metallic component in the module which are negatively charged (-5kV). The moving deposition table then collects a specific ratio of the resulting mat of fibres. The deposition table moves linearly along the three-axis (XYZ), and rotates around the Z-axis (C), as schematically explained in Fig. 2. The resulting deposited fibres on the table, look like the example also shown in Fig. 2.

A specific software was developed to control the various movements of the modules of the electrospinning system [17]. This software has both a manual and an automatic mode, and it allows to create a routine of steps for the modules of the system to follow, such as the flow rate, the position and the linear velocity of both the collecting bands and the deposition table, and the rotational velocity of the latter. The number of repetition cycles can also be defined by the software.

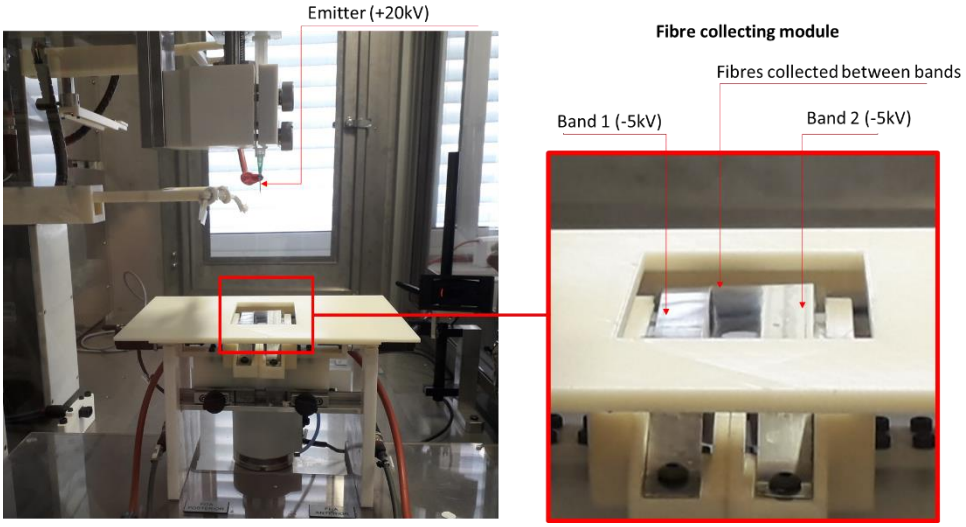

Fig. 1 – Electrospinning setup and its fibre-collecting module.

The experiments (each sample) were conducted with five repetition cycles for each orientation of the deposition table (0º and 90º), this means that, in total, the experimental samples had ten layers of fibres. The resulting meshes were visualized via scanning electron microscopy (SEM, Hitachi TM4000 plus, Japan) at an accelerating voltage of 5 kV. Based on the SEM images, fibre diameter, pore size and distance between the aligned fibres were determined using Image JPro Plus software.

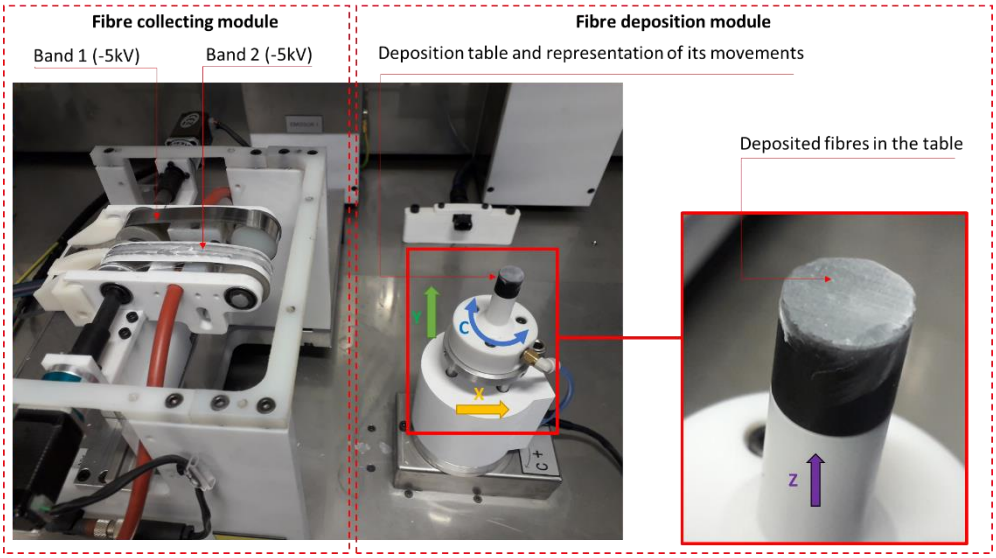

Fig. 2 – Electrospinning setup and its fibre deposition system.

2.3. Design of Experiments (DoE)

Having a better understanding of how the electrospinning equipment's modules work, helps to make a prediction on which factors could have a direct effect on the distance between the fibres and consequently in the mesh porosity. The velocity of the collecting bands (A), as well as the velocity of the deposition table (B), are the two factors that stand out for the ease of control they provide. Moreover, the flow rate (C) is also a defining factor on the distance between the fibres since it controls the amount of fibre that leaves the syringe which are collected by the two bands.

Table 1 – Design of Experiments table.

	Factors			Interactions between factors				Experimental Values		
Experiment	A	B	C	AB	AC	BC	ABC	A (mm/min)	B (mm/min)	C (mL/h)
1	-1	-1	-1	1	1	1	-1	2000	250	2
2	1	-1	-1	-1	-1	1	1	6000	250	2
3	-1	1	-1	-1	1	-1	1	1000	500	2
4	1	1	-1	1	-1	-1	-1	6000	500	2
5	-1	-1	1	1	-1	-1	1	1000	125	3
6	1	-1	1	-1	1	-1	-1	4000	250	3
7	-1	1	1	-1	-1	1	-1	2000	500	3
8	1	1	1	1	1	1	1	6000	500	3
9	-1	-1	-1	1	1	1	-1	1000	500	2
10	1	-1	-1	-1	-1	1	1	5000	500	1,5
11	-1	1	-1	-1	1	-1	1	3000	750	1,5
12	1	1	-1	1	-1	-1	-1	4000	750	1,5
13	-1	-1	1	1	-1	-1	1	2000	500	4
14	1	-1	1	-1	1	-1	-1	4000	500	4
15	-1	1	1	-1	-1	1	-1	3000	750	4
16	1	1	1	1	1	1	1	5000	750	4

The output mesh variables to be evaluated will be the distance between the fibres since the main goal of the present work is to understand how this variable is affected to find an effective way to produce meshes with aligned fibres with controllable spacing between them. The second output variable to be screened is the mesh pore size, which is highly dependent on the previous variable mentioned. Finally, the third output variable will be the diameter of the resulting fibre. The distance between the fibres is the main factor to be analysed because it is highly connected with the size of the pores of the resulting fibre matrix. The pore size is a critical factor for the chondrocytes' migration progress into the scaffold [11-14].

A two-level factorial design was used to generate the DoE. Since there are three factors, 2^3 experiments needed to be conducted; however, to reach more accurate results and to analyse the interaction between elements, replication was used. The full DoE matrix is represented in Table 1, with a total of 16 experiments. The parameter's low and high values were defined based on previous experiments realised in other studies [9-15], such that the difference between the high and low levels would most likely have a statistical impact.

2.4. Theoretical Model

Theoretically analysing the entire process of the electrospinning system is fundamental to have a general idea of the output results, if no outside factors were influencing. Thus, a mathematical function was developed, taking into account the variables of the electrospinning process; flow rate (F), the velocity of the collecting bands (V_{bands}), and velocity of the deposition table (V_{table}) -, to calculate the distance between the fibres deposited in the table.

Consider that the polymer used on the experiment is released from the syringe at a constant velocity, calculated as shown in Eq. (1).

$$V_{fiber} = \frac{F}{\pi \cdot r_{needle}{}^2} \quad \text{[mm/min]} \tag{1}$$

The collecting bands have a width of 12 mm each, as well as the distance between them. Thus, the total width (W) available for the deposition is 36 mm. Considering that the velocity of the collecting bands is zero, the time it takes to deposit a thread of fibre ($t_{deposition}$) can be calculated by Eq. (2).

$$t_{deposition} = \frac{W}{V_{fiber}} \quad \text{[min]} \tag{2}$$

Having the time each segment of fibre takes to be deposited on the collecting bands, it is possible to calculate the distance between the fibres on the collecting bands (S_{bands}) by multiplying the time of deposition with the velocity of the collecting bands, as shown in Eq. (3).

$$S_{bands} = V_{bands} \cdot t_{deposition} \quad \text{[mm]} \tag{3}$$

In order to calculate the distance between the deposited fibres on the deposition table, since its velocity is a parameter that can be controlled, a simple multiplication of the latter Eq. (3) by the time it takes to deposit the fibres on the collecting bands should result in the distance between the fibres on the deposition table – Eq. (4).

$$S_{table} = \frac{S_{bands}}{V_{bands}} \cdot V_{table} \quad \text{[mm]} \tag{4}$$

This theoretical model was tested in Matlab to see if it can predict the behaviour of the resulting distance between the fibres. For an analysis on how each variable affects the result maintaining the other parameters constant, it was conducted a graphical interpretation of the problem, represented in Fig. 3. The graphs show that the velocity of the collecting bands does not have any effect on the distance between the fibres collected by the deposition table. This makes sense since when the fibres are on the collecting bands, the only factor that should affect the distance they will have on the deposition table is the velocity of the latter. The faster the table moves the fewer fibres it collects, thus, the bigger the distance between them.

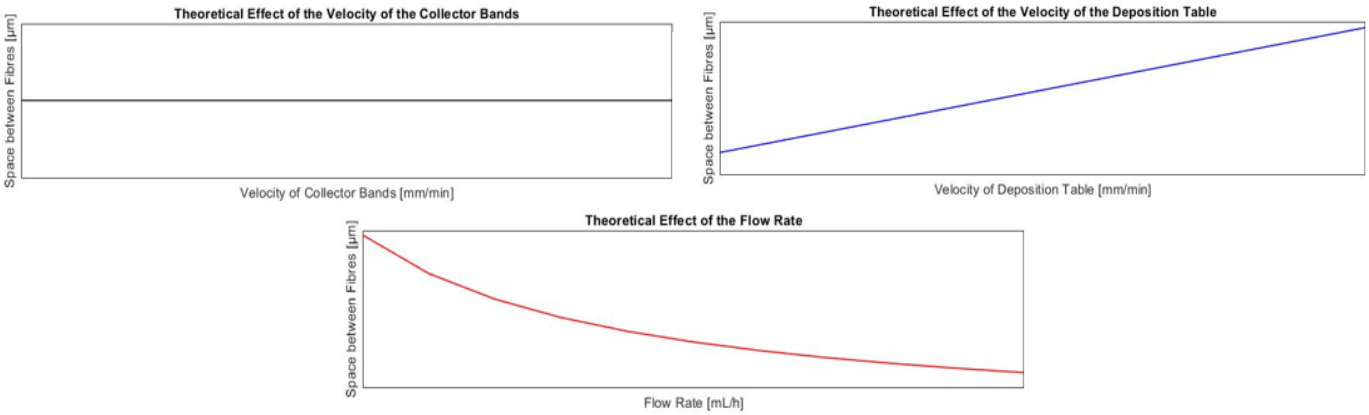

Fig. 1 – Theoretical model's response to input variations (left) and its response to random inputs generated by Matlab (right).

3. Results and Discussion

3.1. Statistical Analysis

Using ImageJ, and after defining the right scale for the SEM image, ten measurements of the distance between the most parallel aligned fibres at 0º and 90º were made (Fig. 4).

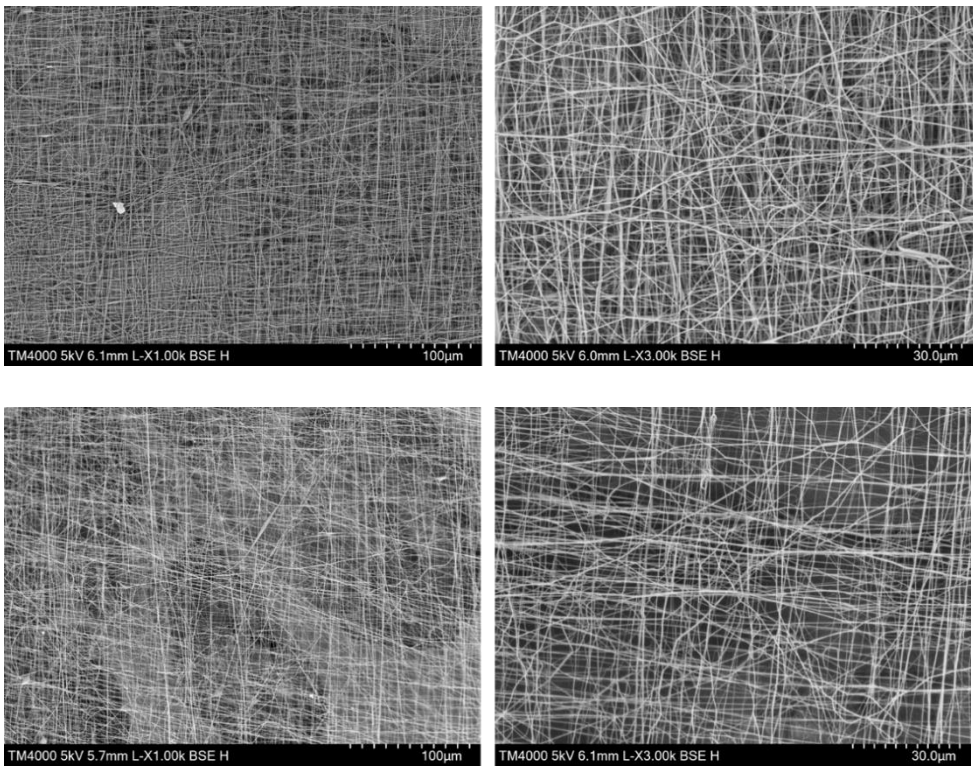

Fig. 4 – Examples of SEM images of two mesh samples: experiment 15 (up) and experiment 2 (down).

With the ten measurements made for each experimental trial, a statistical analysis was conducted using a three-factor ANOVA. Table 2 shows the results for the distance between the aligned fibres. Of all the information presented in the ANOVA table, the primary interest will be focused on "*p-value*", because this is the exact significance level of the factors. If $p<0.05$ then the effect is said to be significant.

Table 2 – ANOVA table for the distance between the aligned fibres (SS- sum-of-squares; df- degrees of freedom; MS- mean squares; F- F ratio).

Factors & Interactions	SS	df	MS	F	p-value
V_{bands} (A)	415,906	5	83,181	3,429	0,007
V_{table} (B)	421,222	3	140,407	5,788	0,001
F (C)	588,885	3	196,295	8,092	0,000
$V_{bands} \cdot V_{table}$ (A x B)	283,062	15	18,871	0,778	0,699
$V_{bands} \cdot F$ (A x C)	1099,347	15	73,290	3,021	0,001
$V_{table} \cdot F$ (B x C)	1125,434	9	125,048	5,155	0,000

Analysing the table presented, it can be concluded that all three independent factors have significance ($p<0.05$) in the resulting distance between the fibres. Moreover, the interactions between the flow rate (F) and the V_{bands}, as well as between V_{table} and the flow rate, also show significance in the results. The next step is to understand precisely how, and how much, the factors, and the interaction between them, influence the results. To do that, the measured values of the distance between the fibres were processed to produce main effect plots and interaction plots, represented in Figs. 5 and 6, respectively.

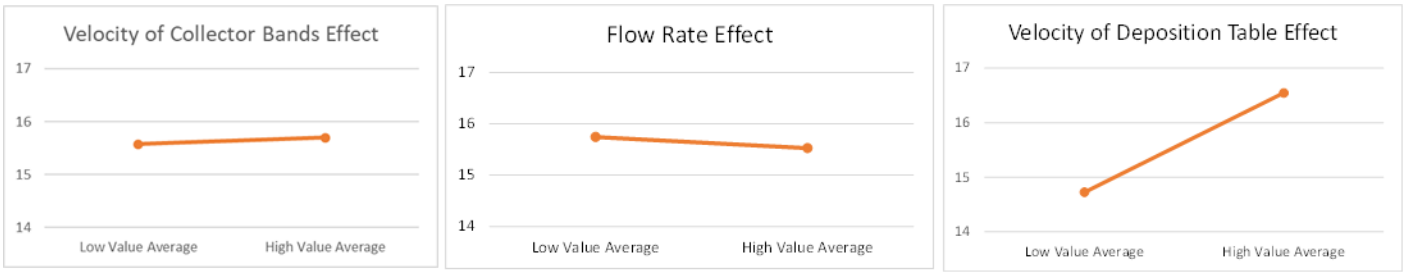

Fig. 5 – Effects of the input parameters on the distance between the aligned fibres

The values presented in Fig. 5 are the means at each level (high/low) under consideration for the parameters, stated in the DoE. Each graph has two points connected by a solid line. The steeper the gradient of the line, the more significant the difference between the two means and, consequently, the higher the influence of the factor. Thus, it can be concluded that the element that has the most impact on the distance between the fibres is the velocity of the deposition table. When increasing the velocity of the deposition table, the distance between the fibres also increases, which was expected. The flow rate has a negative effect, as it can be seen by the slope of the line; when increasing its value, the distance between the fibres will decrease, which was also expected.

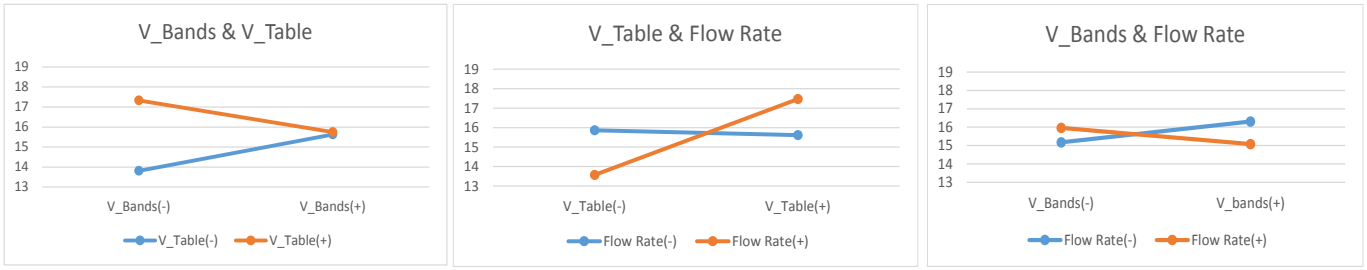

Fig. 6– Interaction plots for the distance between the fibres.

The interaction plots, shown in Fig. 6, give indicators as to how the factors affect the output parameters in combination with each other. The indication is provided by the slope of the 2 lines of each plot, such as the less parallel the lines are, the more likely there is to be a significant interaction between the factors.

Regarding the first interaction plot (V_{bands} and V_{table}), since line V_{table} (+) is, in general, higher than V_{table}(-), it can be concluded that the main effect should be expected in this factor, such that high values of the table's velocity leads to

a higher distance between the fibres. This states that when the factors interact, the dominant factor is the velocity of the deposition table. Even though there is an interaction between the two factors, as the graph proves, the ANOVA table states it is not significant for the results.

There is an interaction between the V_{table} and the flow rate since the lines are not parallel at all. Since the values for the Flow rate (-) are not higher or lower than the values of the Flow rate (+), there is no main effect for flow rate when in combination with the velocity of the deposition table. This is because the velocity of the deposition table shows, in general, a higher impact on the results than the flow rate.

The same analysis was conducted for the fibre diameter. Table 3 contains the results of the ANOVA calculations and it can be concluded that both the velocity of the collecting bands and the flow rate have some significance on the resulting diameter of the fibres. Moreover, both the interactions between the flow rate (F) and the V_{bands}, and the V_{table} and the V_{bands}, also have significance.

Table 3 – ANOVA table for fibre diameter (SS- sum-of-squares; df- degrees of freedom; MS- mean squares; F- F ratio).

Factors & Interactions	SS	df	MS	F	p-value
V_{bands} (A)	0,088	5	0,018	5,574	0,001
V_{table} (B)	0,018	3	0,006	1,881	0,138
F (C)	0,038	3	0,013	3,983	0,010
$V_{bands} \cdot V_{table}$ (A x B)	0,135	15	0,009	2,831	0,001
$V_{bands} \cdot F$ (A x C)	0,131	15	0,009	2,759	0,001
$V_{table} \cdot F$ (B x C)	0,025	9	0,003	0,884	0,543

As it can be seen in Fig. 7, the parameter that has a more significant influence in the fibre diameter is the flow rate ($p<0.05$), as it is the line with the highest slope. The V_{bands} also shows a significant effect on the fibre diameter, increasing the value of the diameter as V_{bands} also increases. The parameter indicating the least amount of influence, and according to ANOVA, not presenting any significance, is the V_{table}.

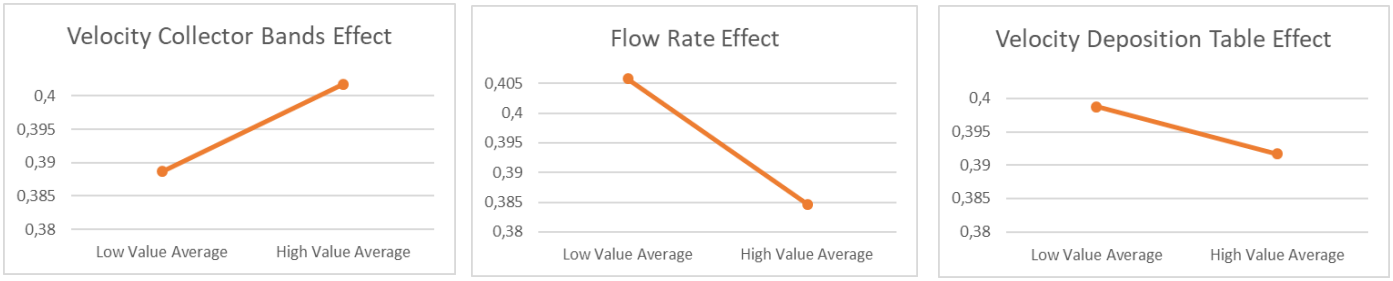

Fig. 7 - Effects of the input parameters on the fibre diameter.

Analysing the interaction plots in Fig. 8, it can be deduced that the flow rate interacts energetically with the velocity of the collecting bands; however, the main effect, when the two parameters interact, is expected to be the V_{bands}.

The lines in the plot of flow rate and V_{table} do not cross each other, which leads to the idea that, if there is an interaction between the two factors, it is very tiny. The ANOVA table shows that there is no significance in the interaction between these two factors, which was expected since, by the time the fibres arrive at the deposition table, the diameter is already defined.

In the plot regarding the interaction between the V_{bands} and V_{table}, the lines come very close to crossing each other, which leads to consider there should be an interaction between the two factors, however, not significant.

The three-factor ANOVA results for the data regarding the pore size are indicated in Table 4. By analysing the data from this table, it can be concluded that, similarly to the results from the distance between the fibres, all the three factors have significance on the results, as well as the interactions between the flow rate and the V_{bands}, and the flow rate and the V_{table}. It was expected that the same factors showed significance since the pore size is highly dependent on the distance between the fibres.

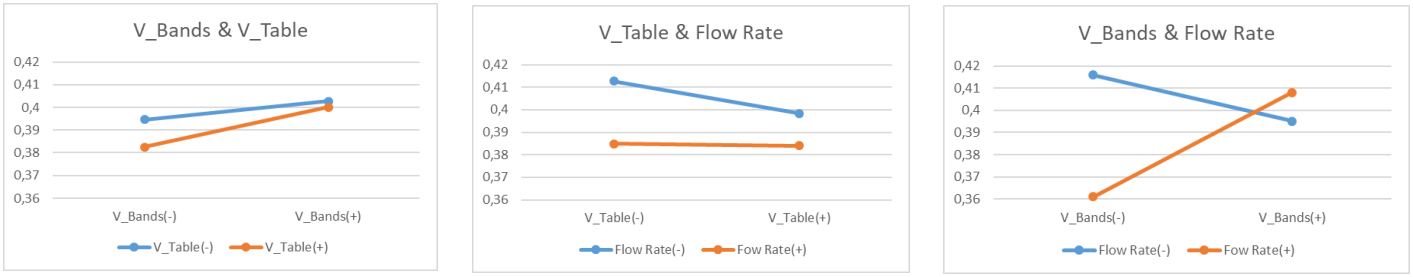

Fig. 8 - Interaction plots for the fibre diameter.

Table 4 – ANOVA table for pore size (SS- sum-of-squares; df- degrees of freedom; MS- mean squares; F- F ratio).

Factors & Interactions	SS	df	MS	F	p-value
V_{bands} (A)	34,051	5	6,810	4,779	0,001
V_{table} (B)	17,758	3	5,719	4,013	0,010
F (C)	29,195	3	9,717	6,818	0,000
$V_{bands} \cdot V_{table}$ (A x B)	6,048	15	0,403	0,283	0,996
$V_{bands} \cdot F$ (A x C)	56,837	15	3,789	2,659	0,002
$V_{table} \cdot F$ (B x C)	32,588	9	3,621	2,541	0,012

As it can be seen in Fig. 9, the parameter that has a more significant influence in the pore size is the velocity of the deposition table, which is in accordance with the results from the effect analysis of the distance between the fibres. The velocity of the bands shows a similar effect on the pore size to the one showed on the distance between the fibres, such that higher values lead to bigger pore sizes and the flow rate shows a positive impact. It should be expected that the parameters behaved similarly to the distance between the fibres, however, that is not the case for the flow rate.

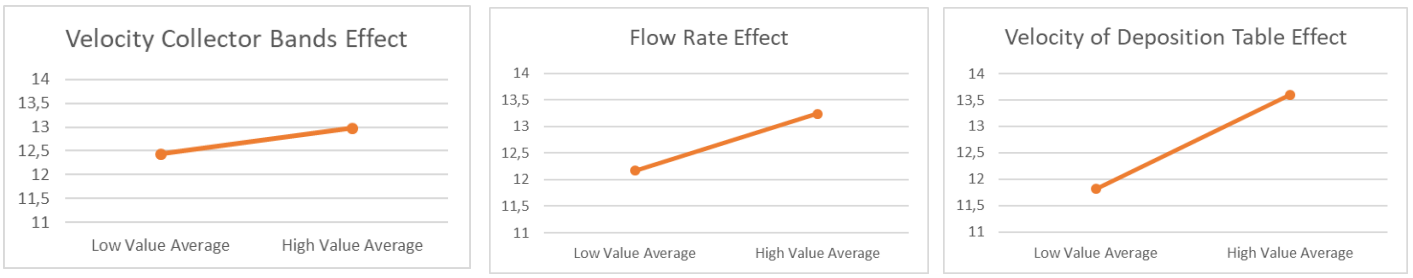

Fig. 9 - Effects of the input parameters on the pore size.

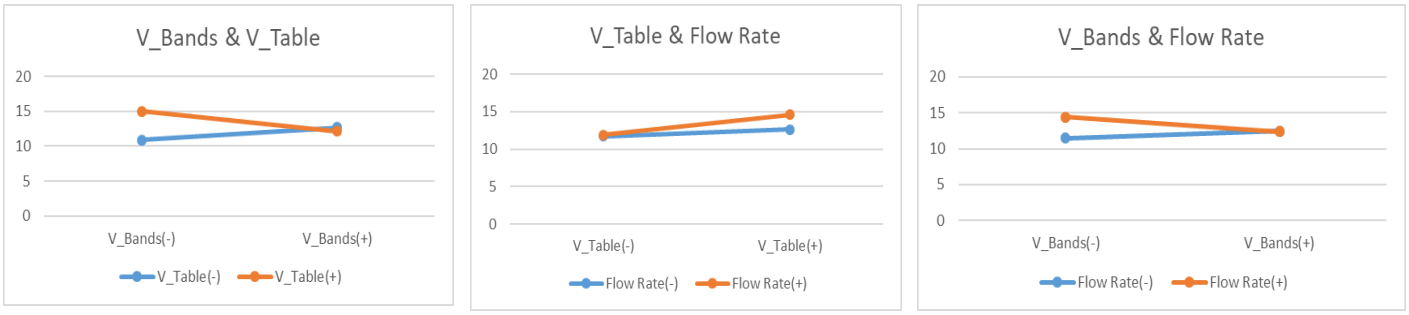

Fig. 10 - Interaction plots for the fibre diameter.

The fact that the measurements of the pore size took in consideration the smallest distance of the pore is probably the reason behind the difference on the calculation of the effect of the flow rate. The velocity of the deposition table, however, presents the higher effect on the pore sizes of the resulting fibre matrices, as it should be expected. As for the interaction between effects – Fig. 10 - it can be concluded that there is an interaction between all the combinations analysed and the most significant one is between the V_{bands} with V_{table}.

3.2. ANOVA Linear Regression vs. Theoretical Model

A linear equation was obtained with the coefficients calculated with ANOVA for each parameter and a constant K, which predicts the distance between the fibres (d_{fiber}) in [μm] after the electrospinning process, having as base the experimental results. In general, the linear regression equation – Eq. (5) - shows sufficiently good results in the prediction of the distance between the fibres, with a standard error for the regression of 4,746, which means the experimental values tend to differ from the ones predicted by the ANOVA model on about 4%.

$$d_{fiber} = 0.1196 \cdot V_{bands} + 1.285 \cdot V_{table} + 0.108 \cdot F - 0.959 \cdot (V_{bands} \cdot V_{table}) - \cdots \\ \ldots - 0.754 \cdot (V_{bands} \cdot F) + 1.272 \cdot (V_{table} \cdot F) - 0.663 \cdot (V_{bands} \cdot V_{table} \cdot F) + K \quad (5)$$

As shown previously, a Matlab theoretical model simulation was conducted to predict how the factors should influence the distance between the fibres. The graph on the left hand-side of Fig. 11 shows the comparison of the theoretical model with the experimental results. The variance on the results is noticeable, which was somewhat expected. While the results from the experiments vary from 10 to 25 µm, the theoretical model range of values goes from 10 to 120 µm. The difference is notorious, and it comes from the fact that, in theory, several external physical factors cannot be accounted. Moreover, the theoretical model assumes the three parameters have the same percentage of relevance on the results, and as seen previously on the statistical analysis, that is not the case.

The model can, however, predict how the variations on the input parameters will affect the distance between the fibres - increase it or decrease it. The theoretical model can also be optimized by adding some adjustment constants that consider the level of significance of each factor. The graph on the right hand-side of Fig. 11 shows the result when the theoretical equation is adapted by taking the effect of parameters into consideration. A significant change can be seen on the outcome results. However, it is still not an accurate prediction since there is a substantial variance between the experimental results and the model's prediction, having an overall average of error of 30%, which is a highly significant value for an error percentage. This outcome is to be expected since electrospinning is a highly complex process, and there are always external factors affecting the results that, in theory, cannot be accounted for. One factor that can be modified to improve the results of the current mathematical model, is the non-consideration that the table velocity is constant throughout its entire displacement, as the table inverts the movement between each deposition of fibres, taking time (acceleration) to reach the programmed velocity, this means that the fibres deposited in reality are at a shorter distance between them because the mean velocity is lower than programmed velocity.

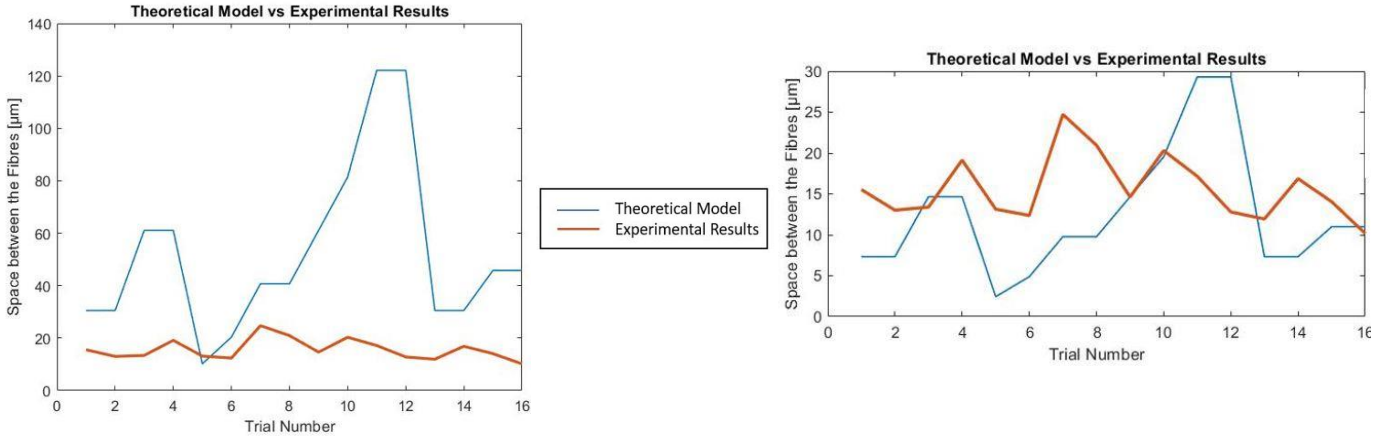

Fig. 11 – Comparison of the theoretical model with the ANOVA model (left) and comparison with the optimized theoretical model with the ANOVA model (right).

4. Discussion

Electrospinning is a simple, unique, versatile, and cost-effective technique widely used for the fabrication of aligned nanofibres [17]. The morphology of the nanofibres is significantly affected by the various parameters such as polymer concentration, viscosity, molecular weight, applied voltage, tip-to-collector distance, and solvent [9-15]. However, in the context of this work, different parameters were analysed to understand if, and how, they would affect specific characteristics of the resulting nanofibres mats. In summary, the three experimental factors, velocity of the collecting bands, the velocity of the deposition table and the flow rate, show significance for the distance between the fibres and the pore size in the obtained electrospun mesh. It is notorious that, for these two output variables, the parameter with higher effect on the results is the velocity of the deposition table, such that higher values of this parameter lead to bigger distance between the fibres and bigger pore sizes. The velocity of the collecting bands also showed similar effects on both the distance between the fibres and the pore size, such that higher values for this parameter lead to higher distance between the fibres and bigger pore sizes. The flow rate showed a negative effect on the distance between the fibres, such that increasing its value leads to smaller distance between the fibres. However, it shows an opposite behaviour on the pore size, having a positive effect. The reason behind these results probably lays on the fact that, electrospinning is sensible to many external factors as temperature, humidity, which cannot be accounted for, could have affected the pore size results. To reduce the randomness of the process, and consequently, the effect of the uncontrollable external factors, more experiments must be performed and accounted for in the statistical analysis.

The model resulting from an ANOVA statistical linear regression, which predicts the result of the distance between the fibres, presented excellent results. However, further optimisation should be conducted to reduce even more the error. This can be achieved by performing more experiments and inserting the resulting data into the ANOVA calculations. The same can be stated for the theoretical model developed. The model should take into consideration on how much each parameter affects the results and maybe, even consider the interaction existent between factors. This can be performed making use of the statistical analysis done throughout this work.

The study on how the various parameters of the electrospinning process affect its results is of great importance, since electrospun nanofibres have found numerous potential applications in almost every field, including enzyme immobilisation, sensing membranes, protective clothing, wound healing and of, course, bone, and cartilage tissue engineering. The study on how to control the alignment and distance of the nanofibres is essential since one of the limitations of the resulting electrospun nanofiber scaffolds is that cells show reduced infiltration into it. Controlling the arrangement, and thus the distance between the fibres is one step closer to the making of 3D scaffolds with the perfect pore sizes for cell infiltration. The ideal pore size for cartilage tissue engineering is not yet determined, however the native cartilage presents chondrocytes sizes around 15 μm [19], which assumes that a pore sizes greater than this value are sufficient to guarantee cell migration. The amplitude of the pore sizes obtained from all DoE experiments done was between 10 μm and 20 μm, which are in the range of the mean chondrocyte sizes reported. The results showed that the parameter with a more significant impact on the distance between the fibres, and consequently pore size, is the velocity of the deposition table. Thus, inserting a moving deposition module, with both linear and rotational movement, to electrospinning equipment is of great help to control the fibre alignment, allowing significant progress for the construction of tissue-engineered cartilage, since it facilitates the replication of the native tissue's complex fibrillar organisation. Thus, allowing to create engineered tissues with anisotropic mechanical properties, like the native tissue of cartilage.

Acknowledgments

The authors acknowledge the financial support through project POCI-01-0145-FEDER-028424-PTDC/EME-SIS/28424/2017, which was funded by the Operational Program for Competitiveness and Internationalization (COMPETE 2020) in its component FEDER and by Science and Technology Foundation (FCT) through the OE budget. The authors also thank to FCT for the PhD grant SFRH/BD/133129/2017.

References

[1] Johnstone B, Alini M, Cucchiarini M, Dodge GR, Eglin D, Guilak F, Madry H, Mata A, Mauck RL, Semino CE, Stoddart MJ. Tissue engineering for articular cartilage repair – the state of the art. Eur Cell Mater. 2013, 25, pp. 248-67.

[2] Bandeiras, C., Completo, A.M.G. Computational Modelling of Tissue-Engineered Cartilage Constructs. Lecture Notes in Computational Vision and Biomechanics, 2020, 35, pp. 203–222.

[3] Bandeiras, C., Completo, A. A mathematical model of tissue-engineered cartilage development under cyclic compressive loading. Biomechanics and Modeling in Mechanobiology, 2017, 16(2), pp. 651–666.
[4] Bandeiras, C., Completo, A., Ramos, A. Influence of the scaffold geometry on the spatial and temporal evolution of the mechanical properties of tissue-engineered cartilage: insights from a mathematical model. Biomechanics and Modeling in Mechanobiology, 2015, 14(5), pp. 1057–1070.
[5] Bandeiras, C., Completo, A. Comparison of mechanical parameters between tissue-engineered and native cartilage: A numerical study. Computer Methods in Biomechanics and Biomedical Engineering, 2015, 18, pp. 1876–1877.
[6] Bandeiras, C., Completo, A., Ramos, A., Ferreira, J.P., Mendes, A.F. Tissue Engineered Cartilage in Unconfined Compression: Biomechanical Analysis. Materials Today: Proceedings, 2015, 2(1), pp. 355–364.
[7] Bandeiras, C., Completo, A., Ramos, A. Compression, shear and bending on tissue-engineered cartilage: a numerical study. Computer Methods in Biomechanics and Biomedical Engineering, 2014, 17, pp. 2–3
[8] Completo, A., Bandeiras, C., Fonseca, F. Comparative assessment of intrinsic mechanical stimuli on knee cartilage and compressed agarose constructs. Medical Engineering and Physics, 2017, 44, pp. 87–93.
[9] N. S. Binulal, A. Natarajan, D. Menon, V. K. Bhaskaran, U. Mony, and S. V. Nair. PCL gelatin composite nanofibres electrospun using diluted acetic acid-ethyl acetate solvent system for stem cell-based bone tissue engineering. J Biomater Sci Polym Ed. 2014, 25, pp. 325-340.
[10] K. Ren, Y. Wang, T. Sun, W. Yue, and H. Zhang. Electrospun PCL/gelatin composite nanofibre structures for effective guided bone regeneration membranes. Materials Science and Engineering C. 2017, 78, pp. 324-332.
[11] Semitela, Â., Girão, A.F., Fernandes, C., ...Completo, A., Marques, P.A.A.P. Electrospinning of bioactive polycaprolactone-gelatin nanofibres with increased pore size for cartilage tissue engineering applications. Journal of Biomaterials Applications, 2020, 35(4-5), pp. 471–484
[12] Girão, A.F., Semitela, Â., Pereira, A.L., Completo, A., Marques, P.A.A.P. Microfabrication of a biomimetic arcade-like electrospun scaffold for cartilage tissue engineering applications. Journal of Materials Science: Materials in Medicine, 2020, 31(8), 69.
[13] Girão, A.F., Semitela, Â., Ramalho, G., Completo, A., Marques, P.A.A.P. Mimicking nature: Fabrication of 3D anisotropic electrospun polycaprolactone scaffolds for cartilage tissue engineering applications. Composites Part B: Engineering, 2018, 154, pp. 99–107
[14] Cortez, S., Freitas, F.L., Completo, A., Alves, J.L. A 3D finite element model to predict the arcade-like collagen structure in a layered PCL scaffold for cartilage tissue engineering. Computer Methods in Biomechanics and Biomedical Engineering, 2017, 20, pp. 47–48
[15] Girão, A.F., Gonçalves, G., Bhangra, K.S., Completo, A., Marques, P.A.A.P. Electrostatic self-assembled graphene oxide-collagen scaffolds towards a three-dimensional microenvironment for biomimetic applications. RSC Advances, 2016, 6(54), pp. 49039–49051.
[16] Meng Q, An S, Damion, RA, Jin Z, Wilcox R, Fisher J, Jones A. The effect of collagen fibril orientation on the biphasic mechanics of articular cartilage. Journal of the Mechanical Behavior of Biomedical Materials (2017).
[17] Completo, A., Marques P. Automated manufacturing of three-dimensional cell matrices with nanofibres of controlled alignment and uniform cell distribution. Patent pending - European Patent: EP21160776.7 de 04/03/2021.
[18] Zheng, R., Duan, H., Xue, J., Liu, Y., Feng, B., Zhao, S., Zhu, Y., Liu, Y., He, A., Zhang, W., Liu, W., Cao, Y., Zhou, G.. The influence of Gelatin/PCL ratio and 3-D construct shape of electrospun membranes on cartilage regeneration. Biomaterials, 2014, 35, pp. 152–164.
[19] Hirsch, M.S., Cook, S.C., Killiany, R., Hartford Svoboda, K.K. Increased cell diameter precedes chondrocyte terminal differentiation, whereas cell-matrix attachment complex proteins appear constant. The Anatomical Record, 1996, 244, 284–296.